HAL
open science

Fast calculation of electromagnetic scattering in anisotropic multilayers and its inverse problem

Giacomo Rodeghiero, Ping-Ping Ding, Yu Zhong, Marc Lambert, Dominique Lesselier

To cite this version:

Giacomo Rodeghiero, Ping-Ping Ding, Yu Zhong, Marc Lambert, Dominique Lesselier. Fast calculation of electromagnetic scattering in anisotropic multilayers and its inverse problem. ENDE 2014, Jun 2014, Xi'an, China. 10.3233/978-1-61499-509-8-151 . hal-01101753

HAL Id: hal-01101753

https://centralesupelec.hal.science/hal-01101753v1

Submitted on 9 Jan 2015

HAL is a multi-disciplinary open access archive for the deposit and dissemination of scientific research documents, whether they are published or not. The documents may come from teaching and research institutions in France or abroad, or from public or private research centers.

L'archive ouverte pluridisciplinaire **HAL**, est destinée au dépôt et à la diffusion de documents scientifiques de niveau recherche, publiés ou non, émanant des établissements d'enseignement et de recherche français ou étrangers, des laboratoires publics ou privés.

Fast Calculation of Electromagnetic Scattering in Anisotropic Multilayers and its Inverse Problem

P.-P. Ding[1] G. Rodeghiero[1] Y. Zhong[2,3] M. Lambert[1] **D. Lesselier**[1]

Cooperative works among
[1] Laboratoire des Signaux et Systèmes UMR 8506 (CNRS-SUPELEC-Univ. Paris-Sud)
[2] presently in Institute of High Performance Computing, Singapore
[3] formerly in National University of Singapore (NUS) [1]

ENDE Xi'an June 2014

1. **Special thanks to X. Chen from NUS**

Electromagnetic modeling of fiber-based composite structures

$\Longrightarrow$

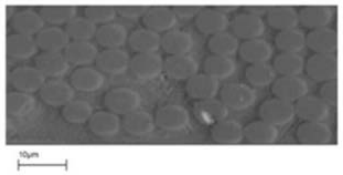

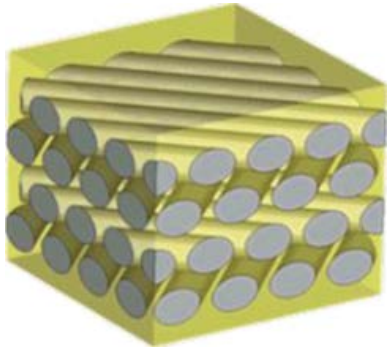

Motivation

- Accurate computational models of complex anisotropic multilayered composite structures
- Robust, fast, end-user's friendly imaging procedures

Forward modeling

$$\bar{\bar{\epsilon}}_r = \text{diag}\left[\bar{\bar{\epsilon}}_{r11} \quad \bar{\bar{\epsilon}}_{r22} \quad \bar{\bar{\epsilon}}_{r22}\right]$$

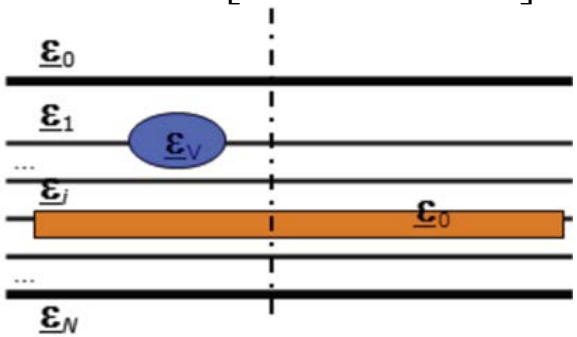

FIGURE: Damaged structure with uniaxial dielectric (glass-based) or conductive (graphite-based) multilayers

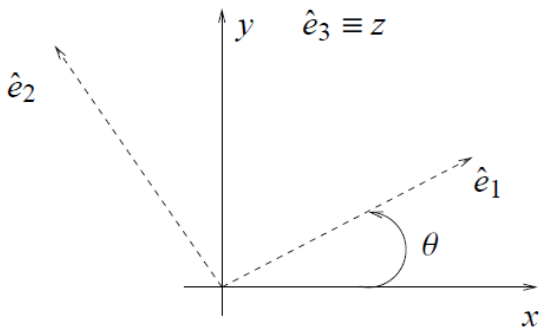

FIGURE: The transformation between the local and global coordinates by rotation matrix

EM response of anisotropic multilayers to distributed sources

The state equation

$$\frac{d}{dz}\bar{\varphi}(z)=\bar{\bar{A}}_n \cdot \bar{\varphi}(z) + \bar{f}(z)$$

based on the 4-component vector :

$$\bar{\varphi}(k_x, k_y, z) = \begin{bmatrix} k_x \tilde{H}_x(k_x, k_y, z) + k_y \tilde{H}_y(k_x, k_y, z) \\ k_y \tilde{H}_x(k_x, k_y, z) - k_x \tilde{H}_y(k_x, k_y, z) \\ k_x \tilde{E}_x(k_x, k_y, z) + k_y \tilde{E}_y(k_x, k_y, z) \\ k_y \tilde{E}_x(k_x, k_y, z) - k_x \tilde{E}_y(k_x, k_y, z) \end{bmatrix}$$

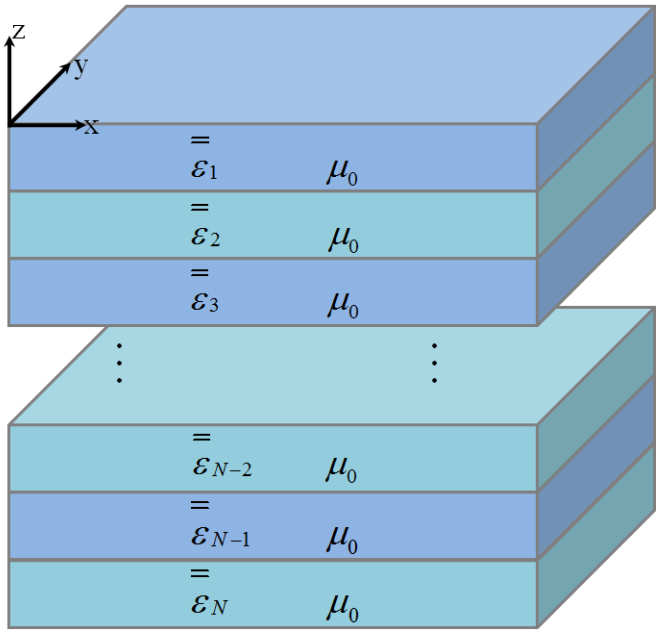

The solution of the state equation

$$\bar{\varphi}(d_{n+1}) = e^{\bar{\bar{A}}_n(\delta_n)} \cdot \bar{\varphi}(d_n) + \int_{d_n}^{d_{n+1}} e^{\bar{\bar{A}}_n(\delta'_n)} \cdot \bar{f}(z')dz'$$

EM response of anisotropic multilayers to distributed sources

The new recurrence equation :

$$\bar{\varphi}\left(d_n\right) = \bar{\bar{\Omega}}_n \cdot \left[\begin{array}{c} \alpha_n \\ \beta_n \end{array} \right]$$

New recurrence relations based on the propagator matrix method

- To efficiently calculate the spectral response of the laminate
- Capable of stably dealing with distributed source along z
- More efficient compared to the traditional Green's function method
- To numerically solve the state equation containing the tangential components of the fields

Two methods for calculating the scattered field

1st method

- Induced current integral equation (ICIE)
- windowing technique
- Padua interpolation-integration technique

2nd method

- Lippman-Schwinger integral formula
- Polarization tensor
- Padua interpolation-integration technique

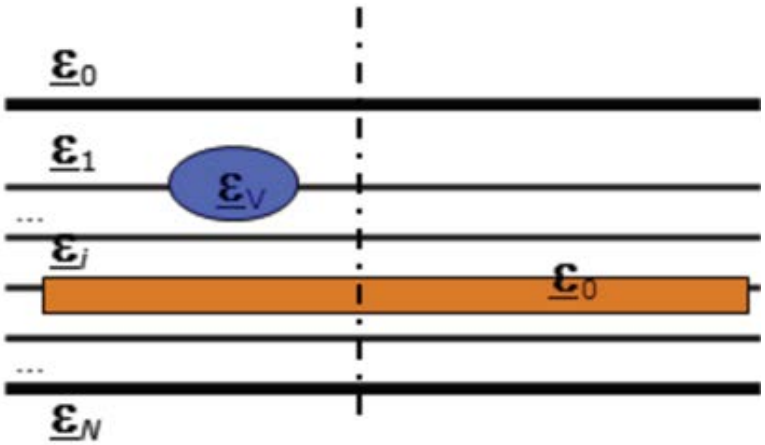

FIGURE: Damaged structure with uniaxial dielectric (glass-based) or conductive (graphite-based) multilayers

Discretization of the integral equation - 1st method

Induced current integral equation (ICIE)

$$\bar{\bar{\chi}}(\mathbf{r}) \cdot \mathbf{E}^{inc}(\mathbf{r}) = \frac{\mathbf{I}(\mathbf{r})}{-i\omega\epsilon_0} - \bar{\bar{\chi}}(\mathbf{r}) \cdot i\omega\mu_0 \int \bar{\bar{G}}(\mathbf{r};\mathbf{r}') \cdot \mathbf{I}(\mathbf{r}') d\mathbf{r}'$$

By MoM

$$\sum_{v=1}^{3} \chi_{u,v;m,n,p} E^{\mathrm{inc}}_{v;m,n,p} = \frac{-1}{i\omega\epsilon_0} \sum_{m',n',p'} I^{(u)}_{m',n',p'} \psi^{(u)}_{m',n',p'}(\boldsymbol{r}_{m,n,p})$$
$$- \sum_{v=1}^{3} \chi_{u,v;m,n,p} \sum_{\kappa=1}^{3} \sum_{p'} \sum_{m',n'} \eta_{v\kappa;p;p';(m-m'),(n-n')} I^{(\kappa)}_{m',n',p'}$$

By fast Fourier transform (FFT)

$$\bar{\bar{\xi}}_{v\kappa;p;p'} = \sum_{m',n'} \eta_{v\kappa;p;p';(m-m'),(n-n')} I^{(\kappa)}_{m',n',p'} = \mathrm{IFFT}\left\{\mathrm{FFT}\left\{\bar{\bar{\eta}}_{v\kappa;p;p'}\right\} \otimes \mathrm{FFT}\left\{{}_{(0)}\bar{\bar{I}}^{(\kappa)}_{p'}\right\}\right\}$$

The techniques for calculating the impedance matrix - 1st method

The impedance matrix :

$$\eta_{\nu\kappa;p;p'}(x,y) = i\omega\mu_0 \int_{\mathcal{D}} G_{\nu\kappa}\left[(x-x'),(y-y');z_p;z'\right]\psi^{(\kappa)}_{0,0,p'}(\boldsymbol{r}')d\boldsymbol{r}'$$

After detouring the integral path to avoid branch cuts or singularites for the integral involving $\widetilde{\eta}_{\nu\kappa;p;p'}(k_x,k_y)$, the DFT of $\overline{\overline{\eta}}'_{\nu\kappa;p;p'}$ (the windowed version of $\overline{\overline{\eta}}_{\nu\kappa;p;p'}$) can be constructed as

$$\begin{aligned}\hat{\eta}'_{\nu\kappa;p;p';\alpha,\beta} &= \frac{1}{4\pi^2\Delta x\Delta y}\exp\left(i\frac{2\pi\alpha}{M_{\mathrm{t}}\Delta x}x_{\mathrm{s}} + i\frac{2\pi\beta}{N_{\mathrm{t}}\Delta y}y_{\mathrm{s}}\right)\\ &\iint_{-\infty}^{+\infty} d\sigma_x^{\mathrm{R}}d\sigma_y^{\mathrm{R}}\ \widetilde{\eta}_{\nu\kappa;p;p'}\left[\sigma_x(\sigma_x^{\mathrm{R}},\sigma_y^{\mathrm{R}}),\sigma_y(\sigma_x^{\mathrm{R}},\sigma_y^{\mathrm{R}})\right]\left|\frac{\partial(\sigma_x,\sigma_y)}{\partial(\sigma_x^{\mathrm{R}},\sigma_y^{\mathrm{R}})}\right| \times\\ &\left\{\sum_{l_1,l_2=-\infty}^{+\infty} e^{i2\pi[l_1(x_{\mathrm{s}}/\Delta x)+l_2(y_{\mathrm{s}}/\Delta y)]}\widetilde{w}\left[\frac{2\pi}{\Delta x}\left(\frac{\alpha}{M_{\mathrm{t}}}+l_1\right)-\sigma_x\left(\sigma_x^{\mathrm{R}},\sigma_y^{\mathrm{R}}\right),\frac{2\pi}{\Delta y}\left(\frac{\beta}{N_{\mathrm{t}}}+l_2\right)-\sigma_y\left(\sigma_x^{\mathrm{R}},\sigma_y^{\mathrm{R}}\right)\right]\right\}\end{aligned}$$

2-D Hamming window

$$\begin{aligned}w(x,y) = &\left\{0.54+0.46\cos\left[\frac{(x-\Delta x/2)\pi}{a}\right]\right\}\\ &\times\left\{0.54+0.46\cos\left[\frac{(y-\Delta y/2)\pi}{b}\right]\right\}\end{aligned}$$

Padua interpolation-integration technique - calculating fast oscillating integrals

- The goal is to compute the I-FT of fast oscillating spectrum in the $k_x - k_y$ plane

$$G(x,y) = \frac{1}{4\pi^2} \iint_{-\infty}^{\infty} \tilde{G}_0(k_x,k_y) e^{\left(ik_x x + ik_y y\right)} \, \mathrm{d}k_x \, \mathrm{d}k_y$$

- Interpolation of the non-oscillating part at the Padua points with Chebyshev's polynomial interpolant

$$\mathcal{L}_n \, \tilde{G}_0 \left(k_x, k_y\right) = \sum_{k=0}^{n} \sum_{j=0}^{k} c_{j,\,k-j} \, \hat{T}_j \left(k_x\right) \hat{T}_{k-j} \left(k_y\right) - \frac{1}{2} c_{n,0} \, \hat{T}_n \left(k_x\right) T_0 \left(k_y\right)$$

  with weights $c_{j,\,k-j}$ computed using [2]

- Fourier transform of Chebyshev polynomials given by

$$\int_{-1}^{1} \hat{T}_n(k_x) \exp(-ik_x x) \, \mathrm{d}k_x$$

  are managed using [3]

2. M. Caliari, S. De Marchi *et al.*, *Numer Algorithms*, **56**, 45-60, 2011
3. V. Dominguez, I. G. Graham *et al.*, *IMA J Numer Anal*, **31**, 1253-1280, 2011

Padua interpolation-integration technique - calculating fast oscillating integrals

Alternative representation as self intersections and boundary contacts of the generating curve $\gamma(t) = (-\cos((n+1)t), -\cos(nt),\ t \in [0, \pi])$

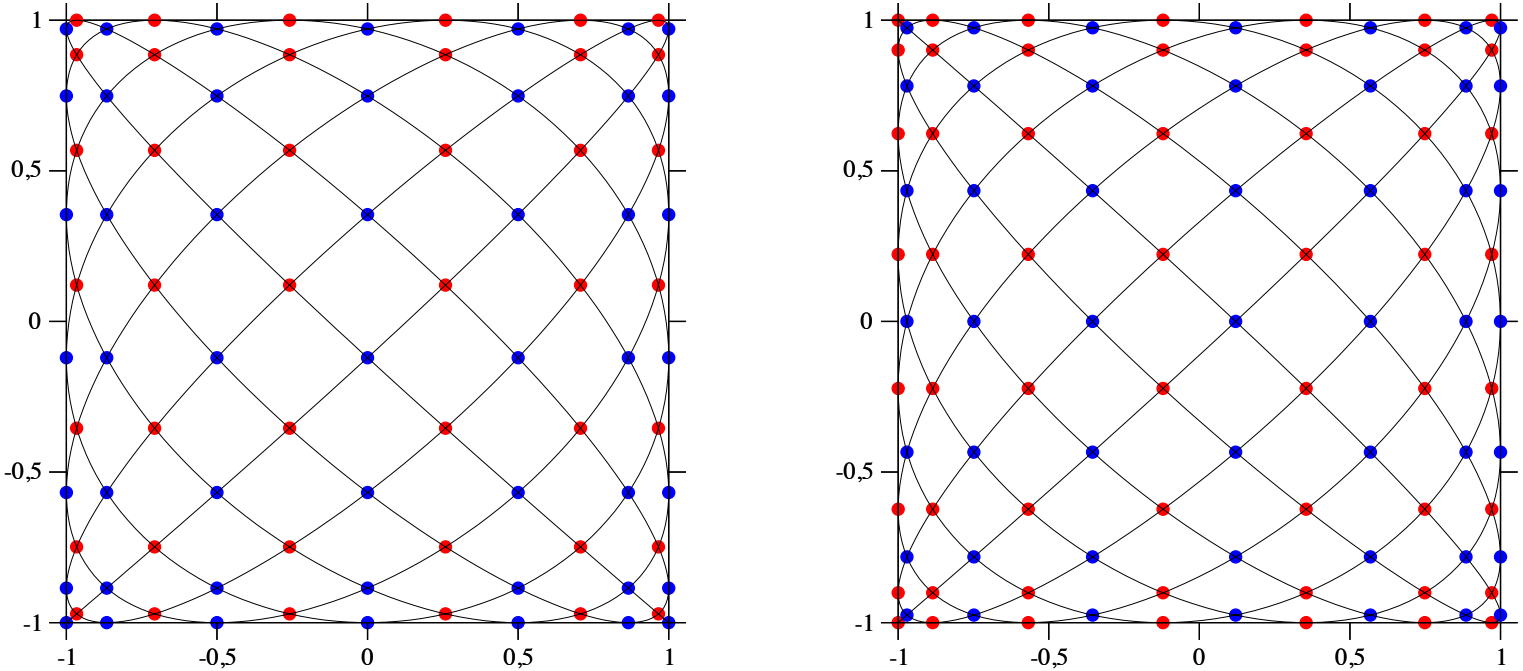

FIGURE: The Padua points with their generating curve for $n = 12$ (left, 91 points) and $n = 13$ (right, 105 points), also as union of two Chebyshev-Lobatto sub-grids (red and blue bullets). Image taken from [5]

M. Caliari, S. De Marchi *et al.*, 5th European Congress of Mathematics - Amsterdam, July, 2008

Fast calculation of EM scattering problems - 2nd method

The Lippman-Schwinger integral formulation

$$\mathbf{E}^{sca}(\mathbf{r}) = i\omega\mu_0 \int \bar{\bar{G}}^{ee}(\mathbf{r},\mathbf{r}') \cdot \bar{\bar{\chi}}(\mathbf{r}') \cdot \mathbf{E}^{tot}(\mathbf{r}')\, d\mathbf{r}'$$

where the contrast function

$$\bar{\bar{\chi}}(\mathbf{r}) = -i\omega\epsilon_0 \cdot \left(\bar{\bar{\epsilon}}_i - \bar{\bar{\epsilon}}_b\right)$$

$\bar{\bar{\epsilon}}_i$ is the permittivity tensor of an inclusion in the composite medium.
$\bar{\bar{\epsilon}}_b$ is the permittivity tensor of the composite medium in the global coordinate system.

The incident field is defined as

$$\begin{aligned} \mathbf{E}^{inc}(\mathbf{r}) &= i\omega\mu_0 \int \bar{\bar{G}}^{ee}(\mathbf{r},\mathbf{r}') \cdot \mathbf{J}_0(\mathbf{r}')\, d\mathbf{r}' \\ &= i\omega\mu_0 \bar{\bar{G}}^{ee}(\mathbf{r},\mathbf{r}') \cdot \beta I l \end{aligned}$$

Asymptotic formulation with polarization tensor - 2nd method

The Lippman-Schwinger integral formulation

When permittivity tensor of the inclusion $\bar{\bar{\epsilon}}_i = \bar{\bar{I}}\epsilon_i$ and its size is small enough, the scattered field can be derived into the asymptotic formulation.

$$\mathbf{E}^{sca}(\mathbf{r}) = i\omega\mu_0 \bar{\bar{G}}^{ee}(\mathbf{r}, \mathbf{r}_m) \cdot \bar{\bar{\varrho}} \cdot \mathbf{E}^{inc}(\mathbf{r}_m)$$

The polarization tensor

The polarization tensor in the local coordinate for the inclusion with volume V is :

$$\bar{\bar{\varrho}} = -i\omega\epsilon_0 V \cdot \begin{bmatrix} \alpha_l & 0 & 0 \\ 0 & \alpha_t & 0 \\ 0 & 0 & \alpha_t \end{bmatrix}$$

$$\alpha_l = \epsilon_{11} \frac{\epsilon_i - \epsilon_{11}}{\epsilon_{11} + L_l(\epsilon_i - \epsilon_{11})}$$

$$\alpha_t = \epsilon_{22} \frac{\epsilon_i - \epsilon_{22}}{\epsilon_{22} + L_t(\epsilon_i - \epsilon_{22})}$$

- L_l and L_t are dependent on the shape of inclusion.
- For a cubic inclusion, $L_l = c \arctan\left(c / \sqrt{1+2c}\right)$ and $L_t = (1 - L_l)/2$, where $c = \epsilon_{11} / \epsilon_{22}$ [6].

6. W. S. Weiglhofer and A. Lakhtakia, *Int. J. Infrared Millimeter Waves*, **17**, 1365–1376, 1996.

Comparison of the scattered field by MoM and COMSOL - 1st Case

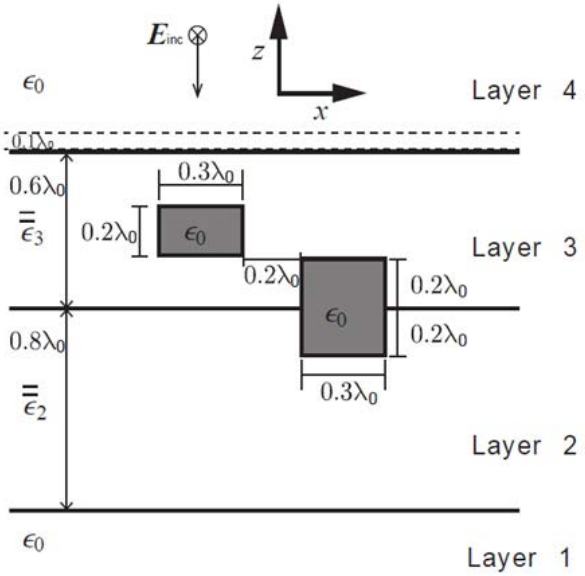

FIGURE: The Configuration of the 1st Case[7]

- freq=6 GHz
- $\bar{\bar{\epsilon}}_2 = \epsilon_0 \,\mathrm{diag}\,[3, 2, 2]$, rotation angle $\theta_2 = 30^\circ$
- $\bar{\bar{\epsilon}}_3 = \epsilon_0 \,\mathrm{diag}\,[4, 2.5, 2.5]$, rotation angle $\theta_3 = 60^\circ$

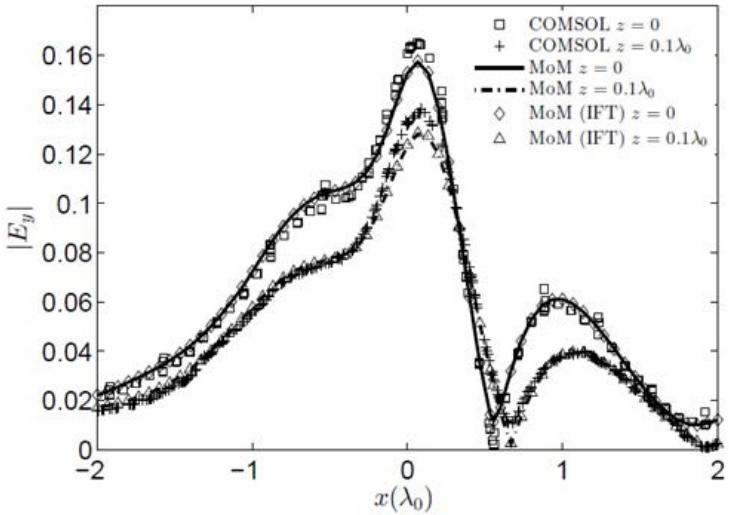

(a) Scattered electric fields along the x-axis.

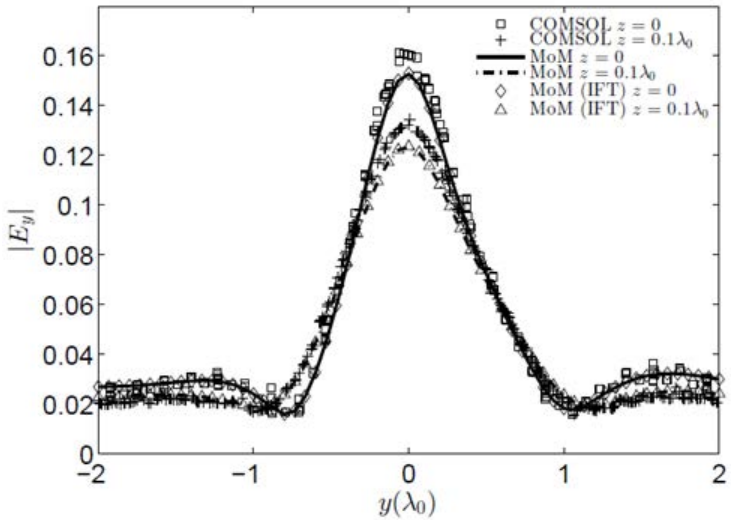

(b) Scattered electric fields along the y-axis.

7. Y. Zhong, P.-P. Ding, M. Lambert, D. Lesselier, and X. Chen, Fast calculation of scattering by 3-D inhomogeneities in uniaxial anisotropic multilayers, *submitted to IEEE Trans. Antennas Propagat.*, 2014.

Comparison of the scattered field by MoM and asymptotic method - 2nd Case

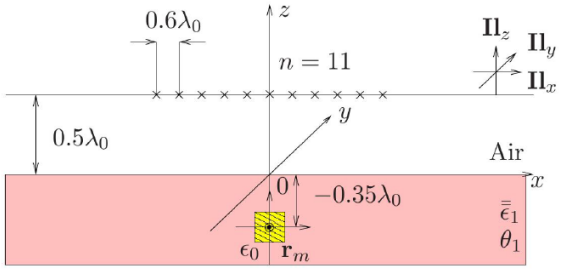

FIGURE: The Configuration of the 2nd Case

- freq=3 GHz
- $\bar{\bar{\epsilon}}_1 = \epsilon_0 \operatorname{diag}[2 + i0.3, 3 + i0.1, 3 +$
- rotation angle $\theta = 60°$
- 11 electric dipole sources with x/y/z polarization
- a cubic air scatterer with side length $0.1\lambda_0$

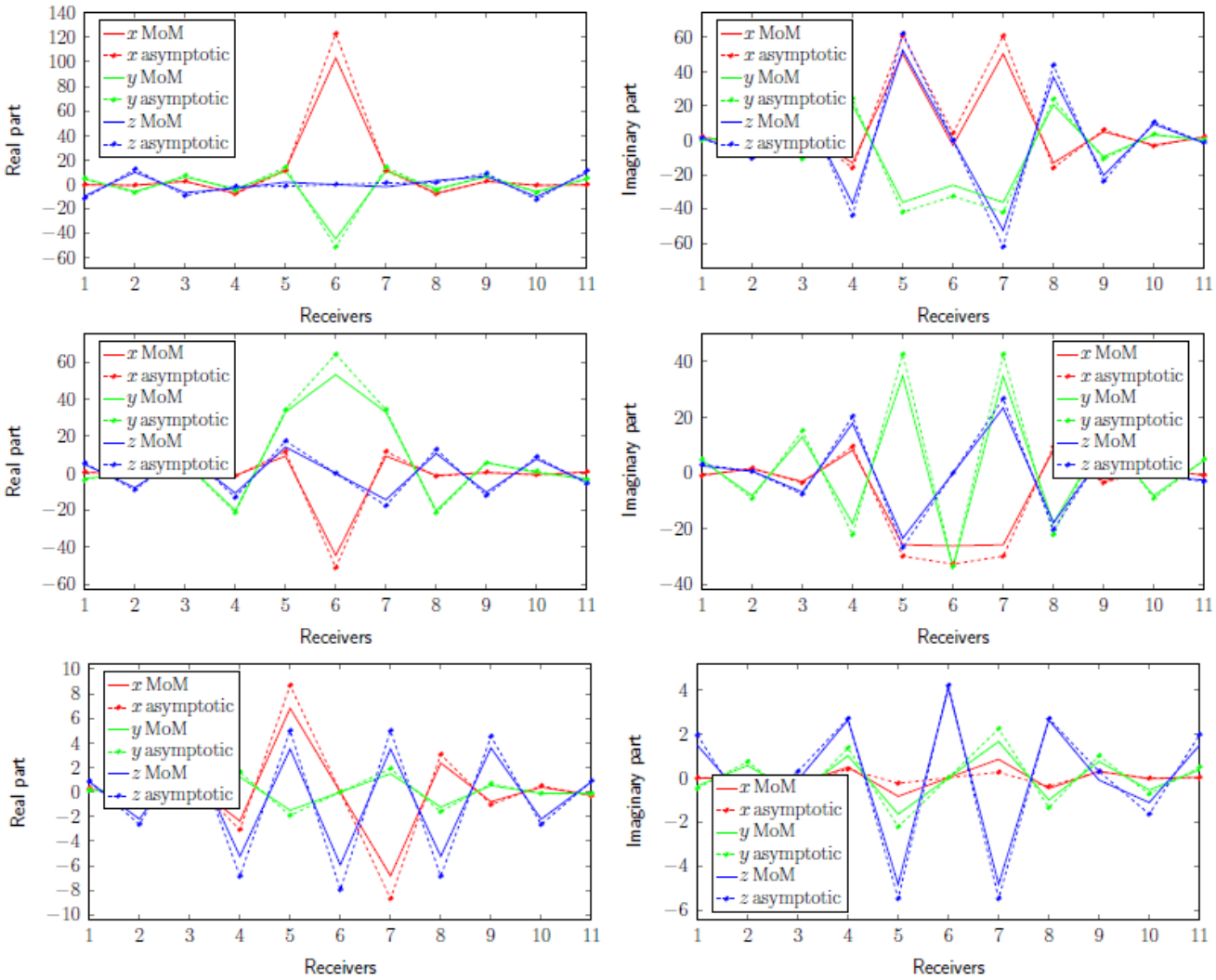

FIGURE: The scattered electric field with sources in x/y/z-polarization

Comparison of the scattered field by MoM and asymptotic method - 3rd Case

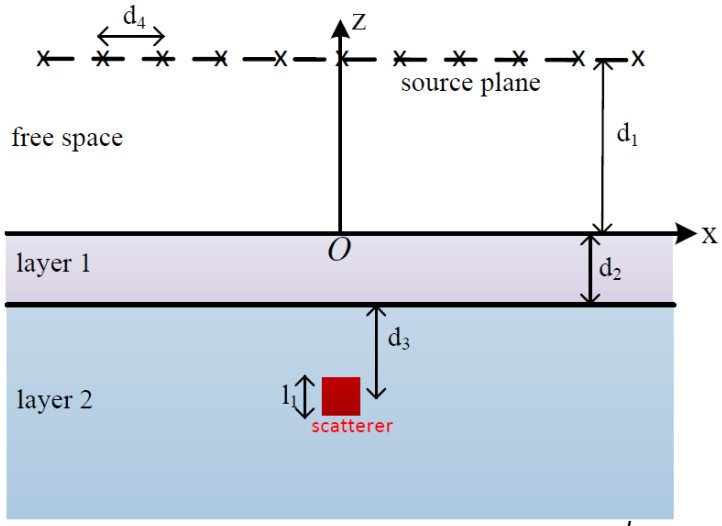

FIGURE: The Configuration of the 3rd Case

- freq $= 3$ GHz
- $d_1 = 0.5\lambda_0$; $d_2 = 0.2\lambda_0$; $d_3 = 0.35\lambda_0$; $d_4 = 0.2\lambda_0$
- layer 1 : $\bar{\bar{\epsilon}}_1 = \epsilon_0 diag\,[2 + i0.3, 3 + i0.1, 3 + i0.1]$; rotation angle $\theta_1 = 60°$
- layer 2 : $\bar{\bar{\epsilon}}_2 = \epsilon_0 diag\,[4.5 + i0.2, 6 + i0.05, 6 + i0.05]$; rotation angle $\theta_2 = 45°$
- 11 electric dipole sources with x polarization
- a cubic air scatterer with side length $0.1\lambda_0$

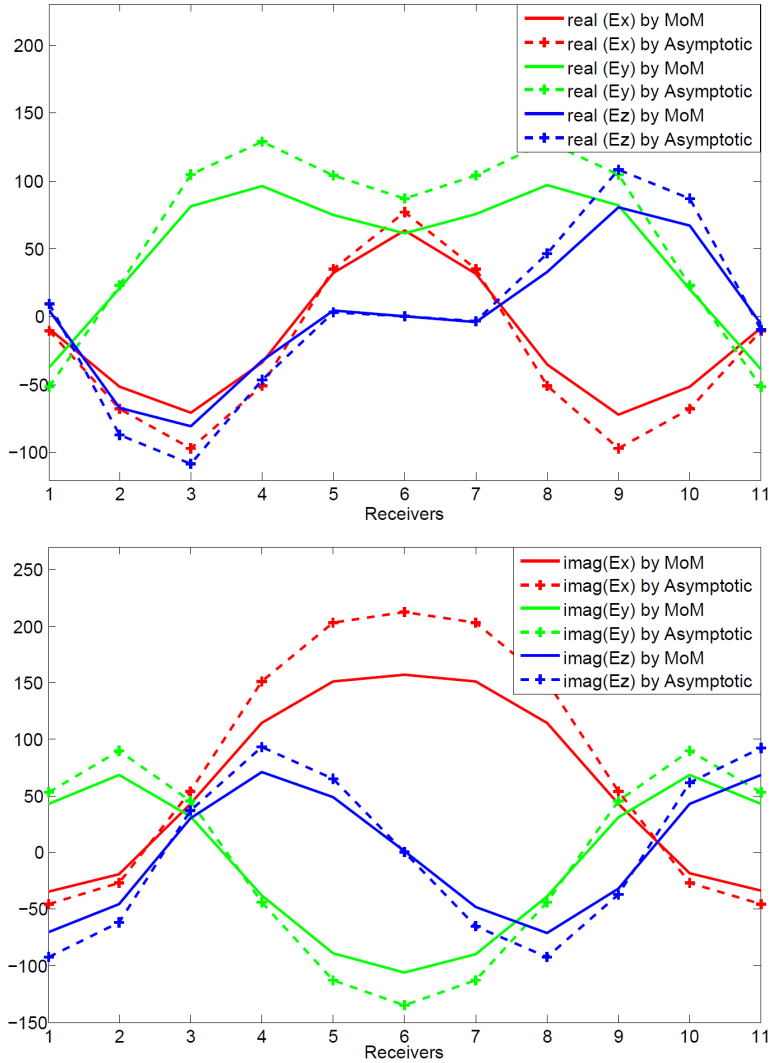

FIGURE: The scattered electric field with the x-polarization source located at $(0, 0, 0.5\lambda_0)$

MUSIC (MUltiple SIgnal Classification) imaging method

Singular value decomposition

$$\mathbf{K} = \mathbf{U}\,\mathbf{S}\,\mathbf{V}^*$$

- Multistatic response matrix **K** maps the currents at the source locations to the scattered fields measured at the detectors.
- Subspace is spanned by the singular vectors corresponding to different singular values.

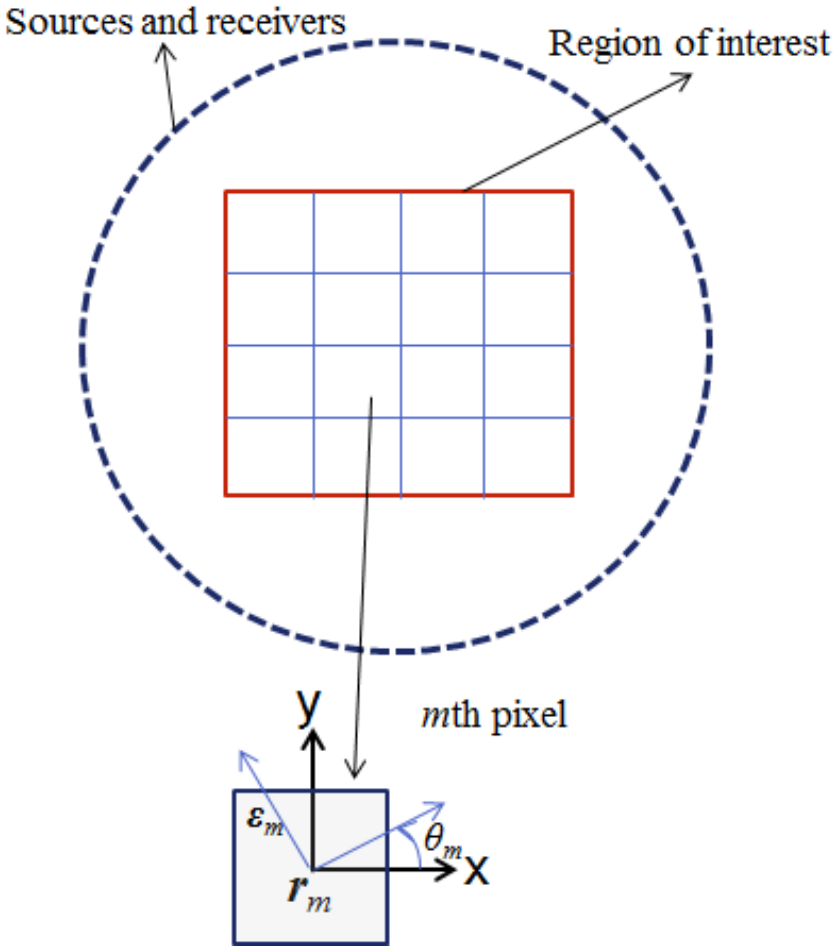

FIGURE: Damaged structure with uniaxial dielectric (glass-based) or conductive (graphite-based) multilayers

MUSIC (MUltiple SIgnal Classification) imaging method

Formulations

Standard MUSIC imaging method [8]

$$\phi(\mathbf{r}) = \frac{1}{\sum_{\sigma_j<\sigma_L}\sum_{v=1}^{3}\left|\bar{u}_j^* \cdot \bar{G}_v(\mathbf{r})\right|^2}$$

Enhanced MUSIC imaging method [9]

$$\phi(\mathbf{r}) = \frac{1}{1-\sum_{\sigma_j>\sigma_L}\left|\bar{u}_j^* \cdot \bar{\bar{G}}(\mathbf{r}) \cdot \bar{a}_{\mathrm{test}}\right|^2}$$

with

$$\bar{a}_{\mathrm{test}} = \arg\max_{\bar{a}} \frac{\sum_{\sigma_j>\sigma_L}\left|\bar{u}_j^* \cdot \bar{\bar{G}}(\mathbf{r}) \cdot \bar{a}\right|^2}{\left|\bar{\bar{G}}(\mathbf{r}) \cdot \bar{a}\right|^2}$$

Choice of σ_L

Exemple for two scatterers $T = 10^3$

- σ_i being ordered from the largest to the lowest value
- A threshold T arbitrarily chosen

$$\sigma_L = T \times \max_i(\sigma_i) \qquad (1)$$

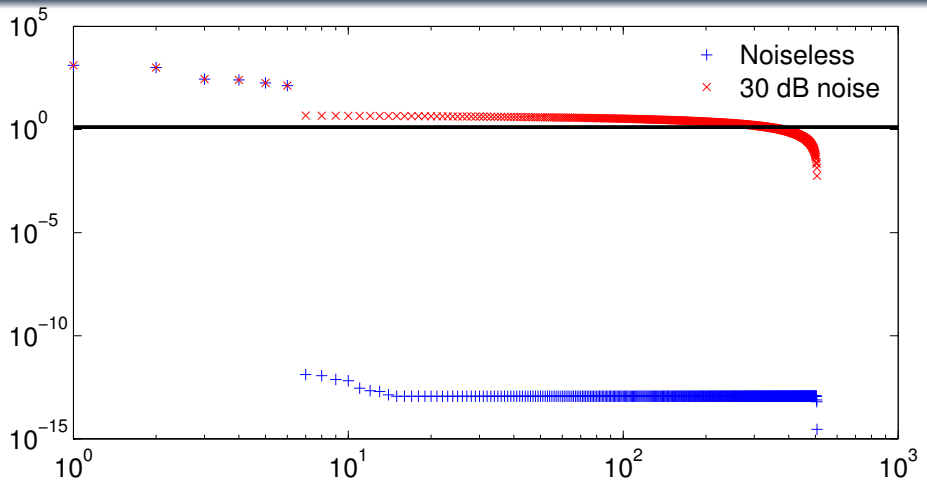

Configuration of interest

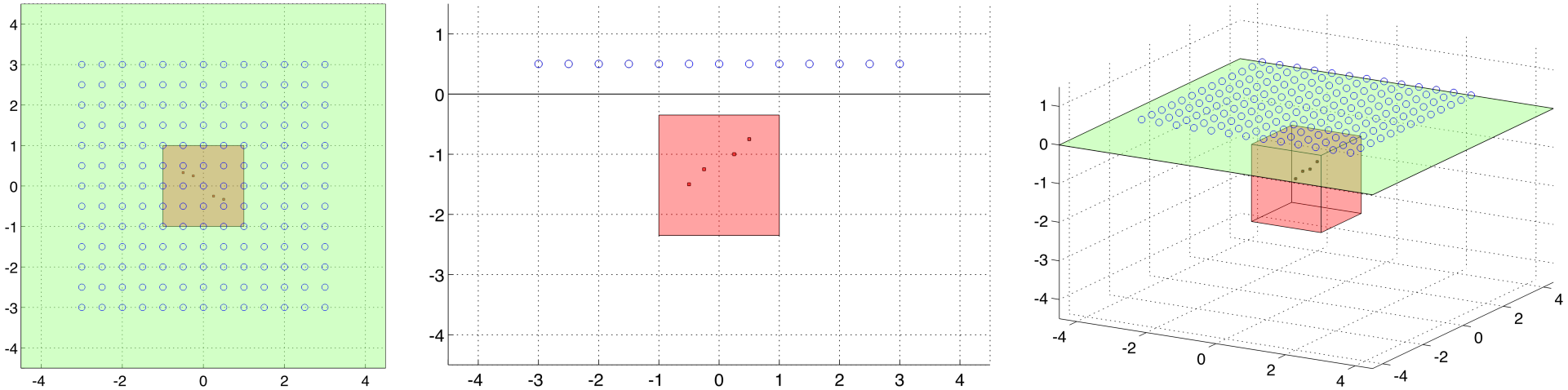

(a) Top view (b) Side view (c) 3D view

FIGURE: Testing configuration

Description of the configuration

Measurement configuration

- location of sources = location of receivers (x/y/z polarization)
- $N_{\text{receivers}} = 13 \times 13$
- z position of receivers : $0.5\lambda_0$
- range of receivers in x-y plane : $[-3\lambda_0, 3\lambda_0]$

Region of interest (ROI)

- $N_{\text{cells}} = 21 \times 21 \times 21$
- range of ROI along z : $[-2.35\lambda_0, -0.35\lambda_0]$
- range of ROI in x-y plane : $[-\lambda_0, \lambda_0]$

The 1st case - one scatterer

plane cut representation

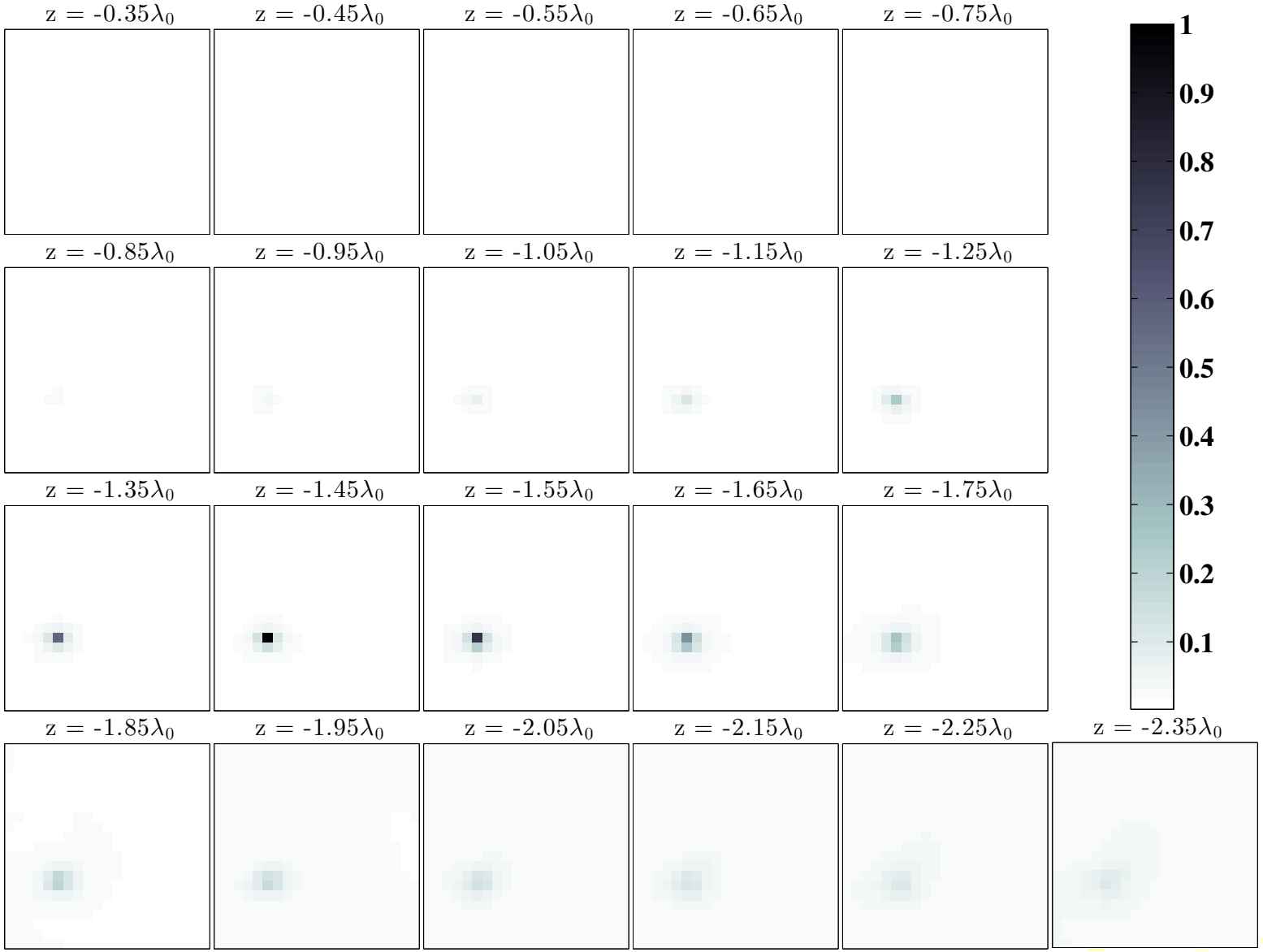

The 1st case - one scatterer

Isosurface = 0.5

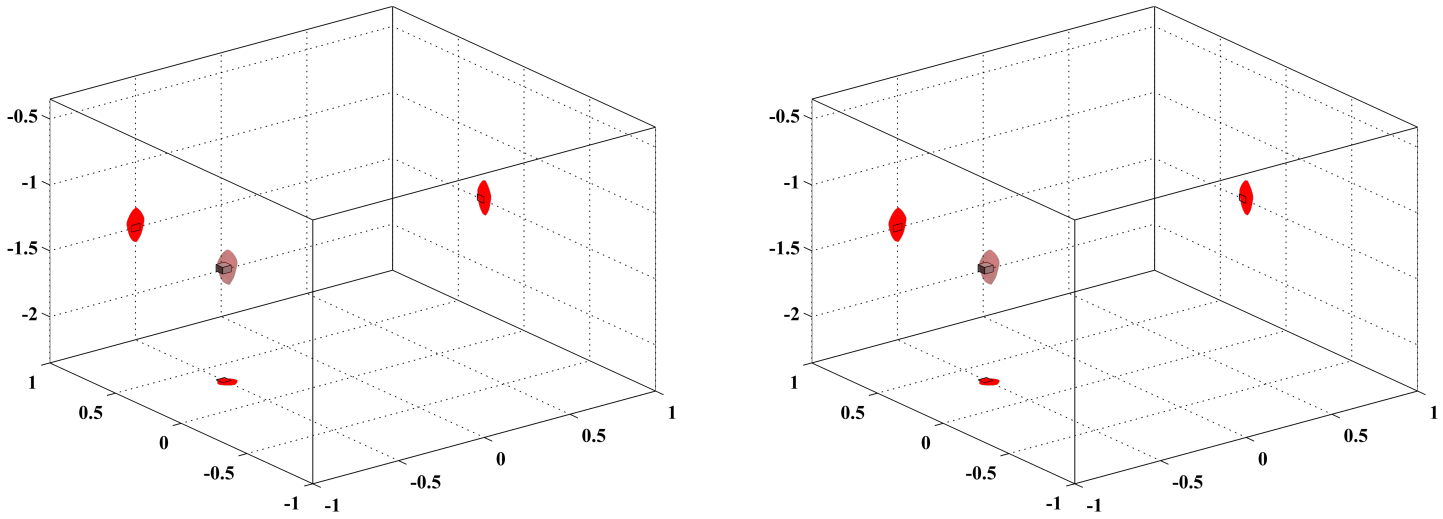

FIGURE: Imaging results by MUSIC for noiseless case (left figure) and 30 dB noisy case (right figure)

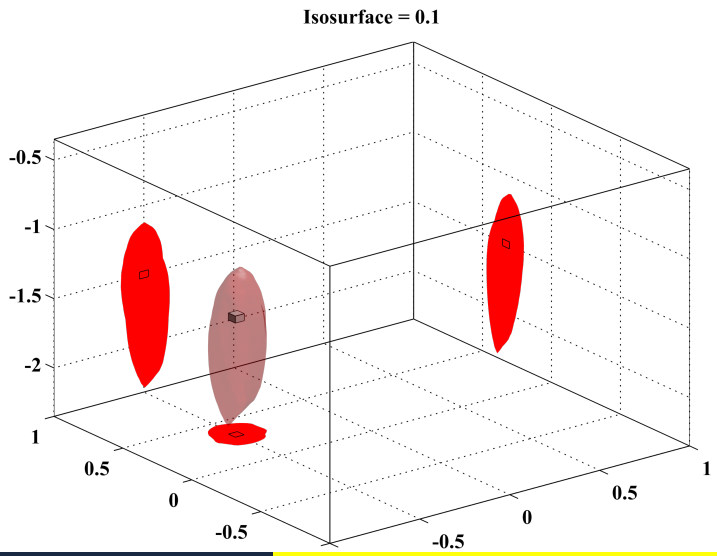

FIGURE: Influence of the choice of the isosurface

The 2nd case - two scatterers

Isosurface = 0.5

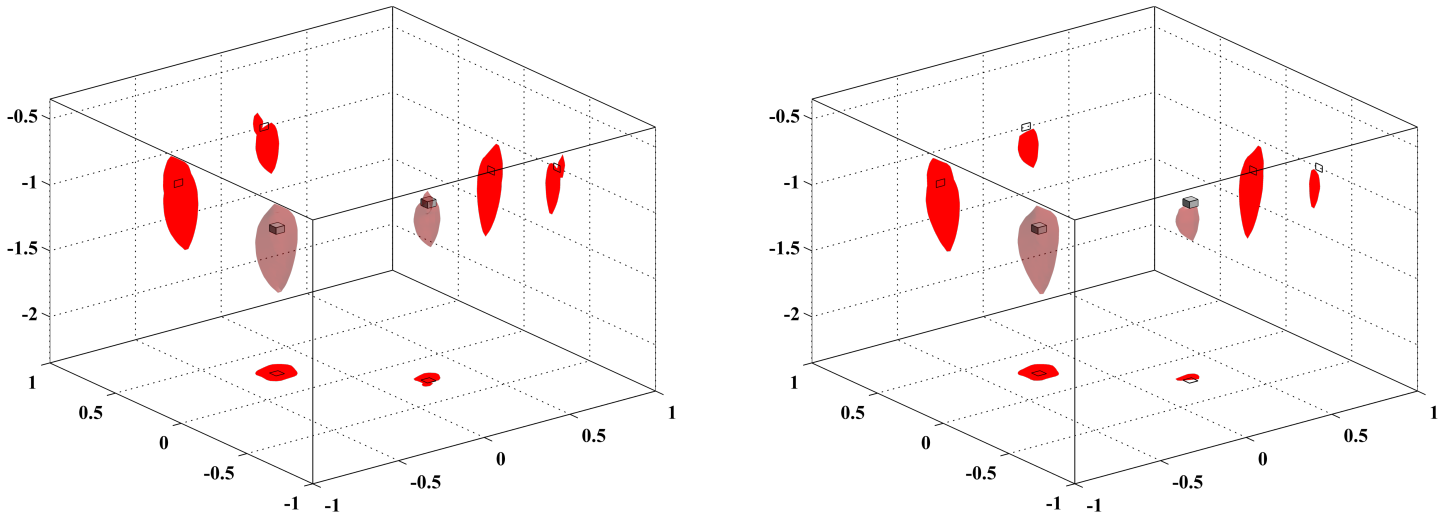

FIGURE: Imaging results by MUSIC for noiseless case (left figure) and 30 dB noisy case (right figure)

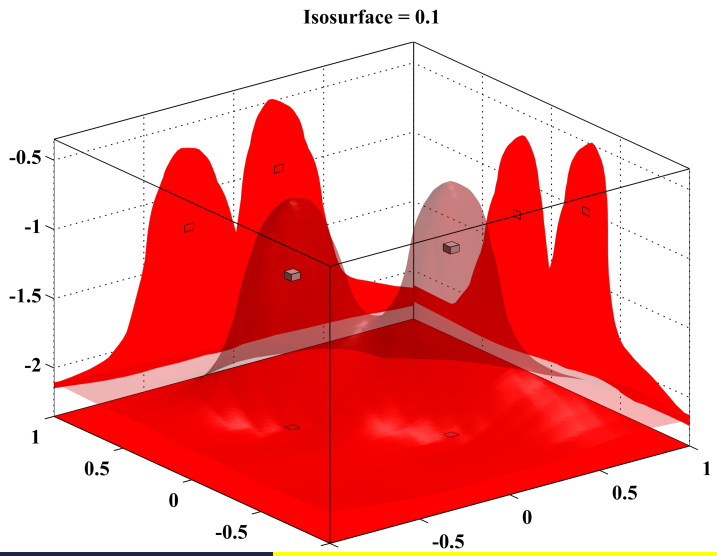

FIGURE: Influence of the choice of the isosurface

The 3rd case - three scatterers

Isosurface = 0.1

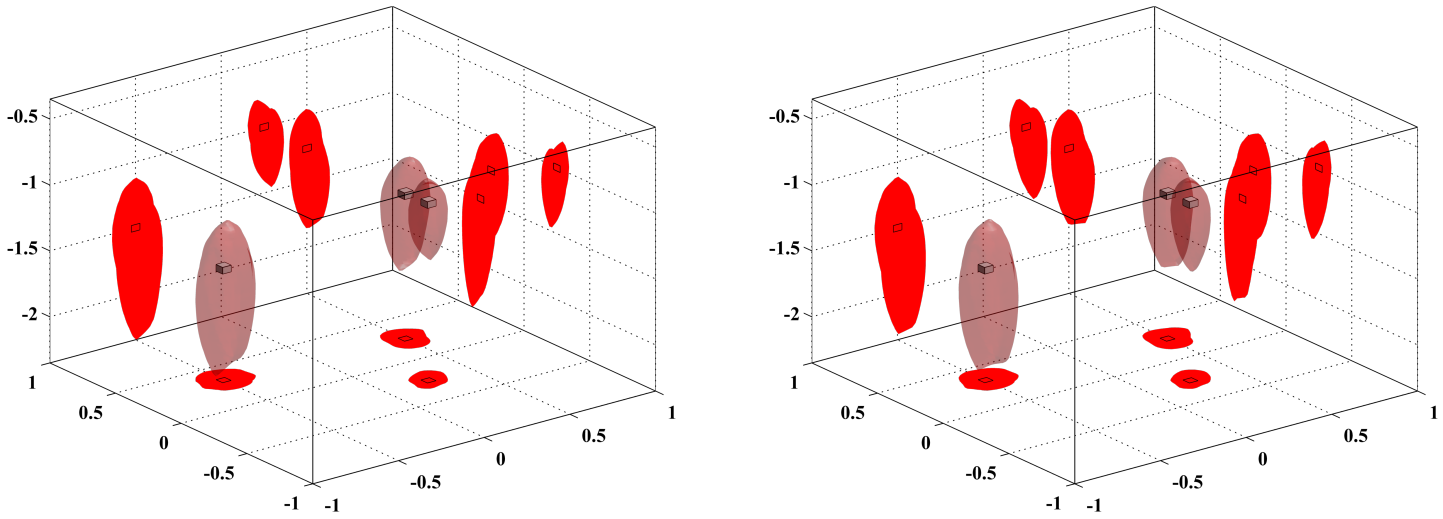

FIGURE: Imaging results by MUSIC for noiseless case (left figure) and 30 dB noisy case (right figure)

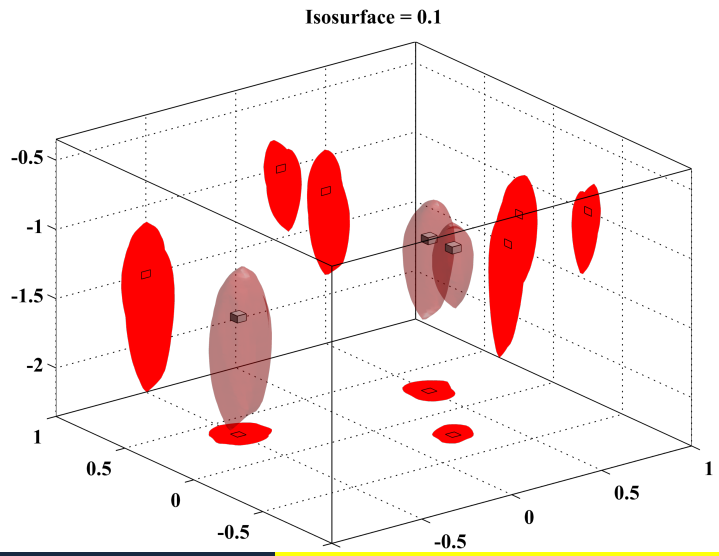

FIGURE: Influence of the choice of the isosurface

The 4th case - four scatterers

Isosurface = 0.1

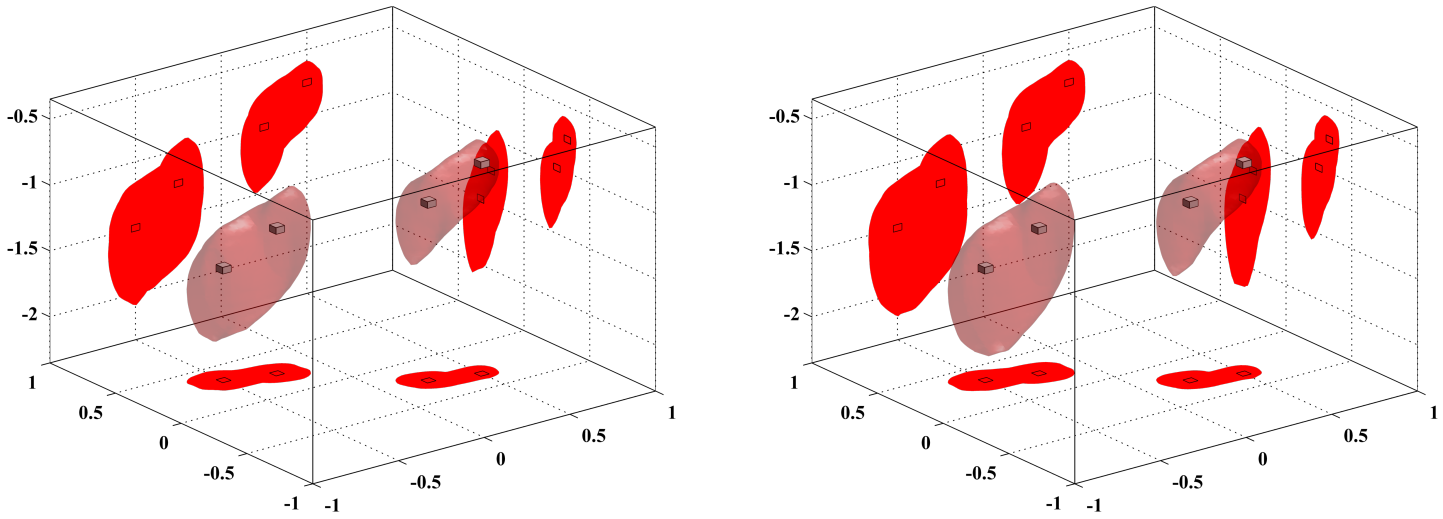

FIGURE: Imaging results by MUSIC for noiseless case (left figure) and 30 dB noisy case (right figure)

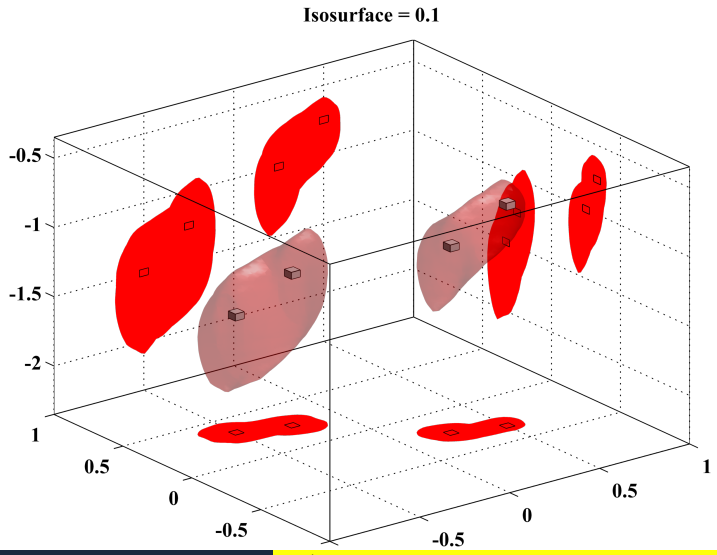

FIGURE: Influence of the choice of the isosurface

Conclusions

Achievements

- Generalized and complete formulation of EM response & Green dyads for undamaged anisotropic multilayers (work at the whole range of frequency for all materials)
- Asymptotic formula-based calculation of EM response for 3-D damaged uniaxial multilayers

Challenges

- To speed up the interpolation and integration for large source-receiver arrays
- To handle delaminations at the interfaces as thin planar defects
- To extend NdT to detecting larger defects by using MUSIC as the first localization tool for non-linearized procedures
- To check the size range of defects possibly detected by the first-order modeling
- To put more endeavor on experiments for practical applications

Thank you & Questions?